Scattering of aligned molecules. The potential energy surfaces for the Kr-O 2 and Xe-O 2 systems

Vincenzo Aquilanti, Daniela Ascenzi, David Cappelletti, Miguel de Castro, and Fernando Pirani

Citation: The Journal of Chemical Physics **109**, 3898 (1998); doi: 10.1063/1.476989
View online: http://dx.doi.org/10.1063/1.476989
View Table of Contents: http://scitation.aip.org/content/aip/journal/jcp/109/10?ver=pdfcov
Published by the AIP Publishing

Scattering of aligned molecules. The potential energy surfaces for the Kr-O_2 and Xe-O_2 systems

Vincenzo Aquilanti and Daniela Ascenzi
Dipartimento di Chimica - Università di Perugia, I-06123 Perugia, Italy

David Cappelletti
Istituto per le Tecnologie Chimiche - Università di Perugia, I-06125 Perugia, Italy

Miguel de Castro and Fernando Pirani
Dipartimento di Chimica - Università di Perugia, I-06123 Perugia, Italy

(Received 23 February 1998; accepted 2 June 1998)

Total integral cross sections for scattering of oxygen molecules on krypton and xenon atoms were measured in the thermal energy range, as a function of the collision energy and under a controlled alignment of the rotational angular momentum of the molecules [Aquilanti *et al.*, Nature, **371**, 399 (1994)]. Data obtained with a ''hot'' effusive molecular beam, which contains fast rotating and randomly oriented O_2 molecules, mainly probe the spherical component of the potential energy surfaces. Experiments with supersonic seeded beams, where the oxygen molecules are cooled at the $K=1$ rotational level and selectively aligned [Aquilanti *et al.*, Phys. Rev. Lett. **74**, 2929 (1995)], probe the anisotropy of the potential energy surfaces. The analysis of the experimental results, based upon close-coupling exact quantum mechanical calculations of the cross sections, provides an accurate characterization of the interactions at intermediate and large intermolecular distances for the Kr-O_2 and Xe-O_2 systems. It is found that the most stable configuration of the two complexes is for perpendicular approach of the rare gas atom, with energies 15.84 for Kr and 17.87 meV for Xe, at intermolecular distances of 3.72 and 3.87 Å, respectively. An adiabatic approximation and a semiclassical description shed light on some general features of the collision dynamics of aligned molecules, in particular on the observed effects of the interaction anisotropy on the glory interference phenomenon. © *1998 American Institute of Physics.* [S0021-9606(98)00334-1]

I. INTRODUCTION

The accurate determination of intermolecular interaction energies is currently an important goal of research in chemical physics. Advances are made possible by experimental developments in molecular beam scattering and laser spectroscopy techniques, which are capable of providing direct information on the involved interactions. The parallel introduction and use of theoretical (quantum and semiclassical) scattering methods permits the quantitative analysis of the available experimental data, while improvements of quantum chemical calculations show perspectives of future accurate description of these weak forces. The wealth of available information has encouraged attempts to quantitatively anticipate parameters for interaction energies via ''correlation'' formulas in terms of fundamental physical properties of the interacting partners— a long standing quest toward modeling of complex systems for which direct experimental and theoretical probing is problematic.

During the past three decades much effort has been addressed to the correct representation of interaction energies in terms of flexible and reliable potential models, the main focus being on systems containing closed shell atoms.[1,2] More recently, attention has been devoted also to systems involving open shell atoms[3,4] (i.e., atoms with total electronic angular momentum different from zero) and molecules of varying complexity.[5] Efforts have been successful in understanding the role played by the anisotropic interactions on the collision dynamics.[6,7]

Modern experimental methods, which involve spectroscopic and molecular beam techniques, represent the richest sources of information on intermolecular interaction potentials. Recent advances in the generation of polarization (orientation and alignment) effects in atoms and molecules[8] (i.e., anisotropic distribution of involved internal angular momenta) open the possibility toward the direct study of *steric* effects which control the evolution of several chemical and physical phenomena.[9] For example, direct information on the strength of the interaction anisotropy and on its role on the collision dynamics can be extracted from scattering data measured with polarized beams.[3,4,10]

In previous work reported from our laboratory,[11] we have described in detail how seeded supersonic expansions of molecular oxygen represent a natural and facile technique for obtaining alignment of molecular rotations.[12] Such observations opened up the way to prepare molecules with well-defined velocities and alignment ratios, simply by changing the gas carrier composition, and suggested the method to carry out scattering experiments (at thermal energies corresponding to the glory region) between rare gases and oxygen molecules with a controlled molecular alignment. Preliminary results for the Xe-O_2 system[13] have shown remarkable effects both on the smooth component of cross sections and on the glory interference patterns, as the alignment degree

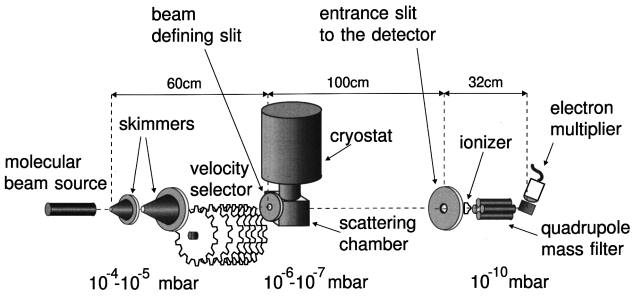

FIG. 1. A schematic view of the experimental apparatus used for integral cross section measurements: the (effusive or supersonic) molecular beam source is shown, together with the velocity selector [eight rotating slotted disks, velocity resolution of ~5% full width at half maximum (FWHM)], the scattering chamber and the quadrupole mass spectrometer. Also indicated are pressure ranges typical of the differentially pumped chambers.

was varied. These observations are of interest because of two main reasons: first of all they represent clear evidence of the fact that total cross sections, which are affected by molecular alignment, will provide information also on the anisotropic part of the intermolecular potential between projectile molecule and target gas atom; second, they prove that scattering experiments can be exploited as a probe of the molecular alignment when the interaction is known. The latter aspect has been recently exploited in the analysis of scattering results for the Xe-N_2 system,[14] to provide an evaluation of N_2 molecular alignment under seeded supersonic expansion.

An accurate determination of the intermediate and long range behavior of the anisotropic intermolecular potential energy surface is presented here for the Xe-O_2 and Kr-O_2 systems. Reported results are the measurements of total integral cross sections as a function of the collision velocity, the focus being on their observable dependence on the controlled polarization degree of the O_2 molecules. The analysis of present data, carried out according to suitable theoretical schemes which link the experimental observables to the interaction potential features, makes use both of essentially exact quantum mechanical close coupling calculations and of approximate methods, such as an adiabatic approach, which has the advantage of gaining insight into the collisional dynamics of aligned molecules, and a semiclassical description which clarifies the underlying physical picture.

In the next section the experimental apparatus is presented, together with a description of the technique employed for the measurement of scattering cross sections. Section III summarizes the theoretical background used in the analysis of scattering results, while results and discussion follow in Sec. IV and concluding remarks are presented in Sec. V. An Appendix illustrates the chosen parametrization for the potential energy surface.

II. EXPERIMENTAL TECHNIQUE AND RESULTS

A. The apparatus

The experimental apparatus employed for the measurements described in this paper is the same as used for the O_2 rotational alignment study[11] and in previous scattering experiments performed with several atomic and molecular beams[3] (see Fig. 1). It consists of a set of differentially pumped vacuum chambers where the molecular beam emerges from a source which can operate under effusive and supersonic conditions, and, after velocity selection, enters into the scattering chamber. The on-line beam intensity is detected by a quadrupole mass spectrometer placed after the scattering region. Changing the source conditions (pressure, nozzle diameter, temperature…) scattering experiments with O_2 in different rotational conditions can be performed in order to probe different portions of the potential energy surfaces.

Total (elastic + inelastic) integral cross sections are obtained through the measurement of the intensity loss of the velocity selected beam as it crosses the scattering chamber, filled with the target gas (Kr and Xe in the present case in the typical pressure range of $10^{-2}-10^{-3}$ Torr) cooled down to liquid or solid air temperature, to decrease the quenching of the glory interference effect by the thermal motion of the target gas. Liquid air is introduced in a cryostat attached to the scattering chamber and solid air is produced by a near-adiabatic evaporation of the liquid by pumping at sufficiently high speed. The cryostat temperatures, which have to be kept very stable in time during the measurements, are monitored by a thermocouple, and found to be ~90 and ~70 K for liquid and solid air cooling, respectively. As previously, the absolute values of total cross sections have been obtained by an internal calibration based on the direct measurements of the gas flowing in the scattering chamber and on the absolute value of He-Ar elastic scattering cross sections reported in Ref. 15.

Under these temperature and pressure conditions of the scattering chamber, no corrections are necessary for the presence of rare gas dimers in the scattering region and the selected beam velocity v practically coincides with the collision velocity of the Xe and Kr-O_2 systems in the center-of-mass frame.

The length of the beam path between the beam defining slit before the scattering chamber and the ionization region (100 cm), together with the radius of the slit (0.35 mm), determines an angular resolution value of the apparatus[16] found to be sufficiently high that any correction due to finite angular resolution is negligible. Therefore the measured data can directly be taken as the true quantum scattering cross sections.

B. Total integral cross sections from an effusive beam of O_2

In these experiments, an effusive beam of molecular oxygen is produced by expanding pure O_2 (source pressure ~3 Torr) from a heated nozzle ($T\sim10^3$ K) of 1.0 mm in diameter; the beam generated from this source contains O_2 molecules in the ground electronic state: they exhibit a manifold of rotational states, with $K=9-13$ as most populated levels, and show a broad velocity distribution.

Absolute total integral cross sections $Q(v)$ for scattering of such a beam by Kr and Xe atoms are reported in Figs. 2 and 3, as a function of collision velocity v in the range 465–2050 for Kr and 560–2230 $m\cdot s^{-1}$ for Xe. As usual, they are plotted as $Q(v)\cdot v^{2/5}$ to emphasize the glory interference pattern (see also Sec. III C), which provides informa-

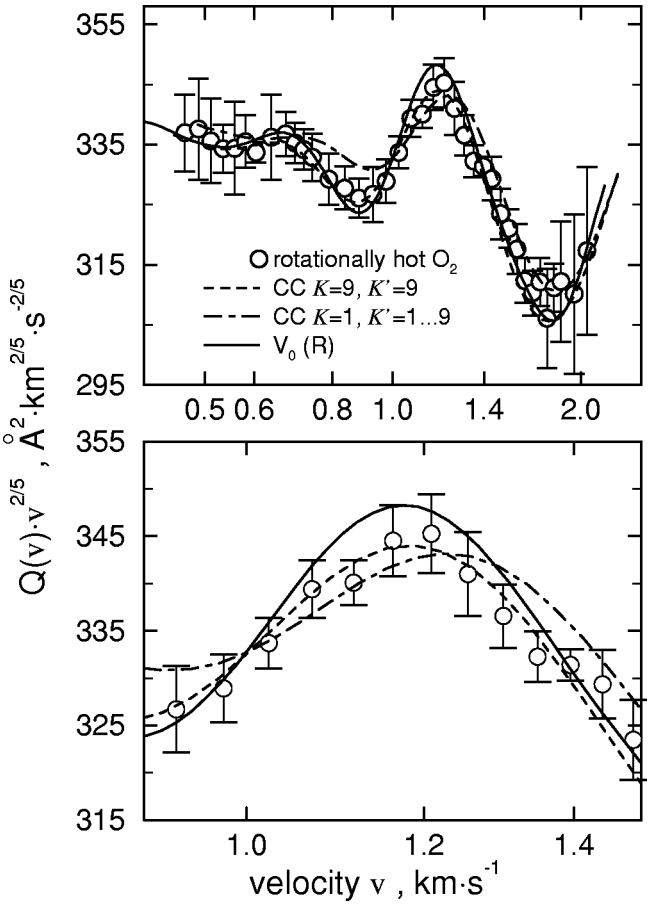

FIG. 2. Scattering of a rotationally ''hot'' effusive beam of O_2 by Kr atoms (most populated rotational levels $K\sim 9-13$): total integral cross section $Q(v)$, multiplied by $v^{2/5}$, is plotted as a function of velocity v (in log scale). Solid line represents calculated cross sections in the atom-atom approximation assuming scattering by a single potential curve, corresponding to the isotropic (spherical) interaction $V_0(R)$ (see Appendix and Table II). Dashed line represents the CC calculations for elastic cross section for the channel $K=9,K'=9$ using the complete PES, while dotted-dashed line is the result of a CC calculation for total cross sections (see text), considering the O_2 molecules randomly oriented in $K=1$. The right panel is a blow up of the glory maximum occurring at highest velocities, shown to compare different calculations.

tion on the interaction potential features of the collision complex. In particular under such experimental conditions, where O_2 molecules are fast rotating, this information concerns mainly the spherical component of the interaction, i.e., the potential resulting from the average over all spatial orientations of the oxygen molecule. Dashed, dotted-dashed, and continuous lines in the figures are the results of calculations to be discussed in the next section.

Similar results, measured using an effusive oxygen beam, had been reported previously;[17] present experiments agree with the older ones, but are of improved accuracy, having been performed with a more stable beam and under higher energy resolution because of the reduction of the target gas motion in the cooled scattering chamber.

C. Total integral cross sections from supersonic seeded beams of O_2

Supersonic seeded beams of molecular oxygen have been produced by expanding diluted (containing in all cases

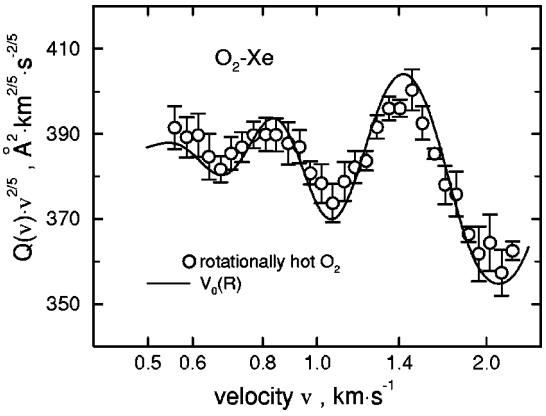

FIG. 3. Total integral cross sections, as in Fig. 2, for scattering of a rotationally ''hot'' effusive beam of O_2 by Xe atoms. Solid line represents calculations in the central field approximation, whose potential corresponds to the isotropic (spherical) interaction $V_0(R)$ (see Appendix and Table II).

2.5% of O_2) gas mixtures from a 100 μm nozzle at the total pressure of 800 Torr. Carrier gases like Ne, He and H_2 have been used, either pure or in mixtures, whose compositions have been varied to cover a wide range of peak velocities $v_{\max}$ of the seeded beams, from 800 to 2300 m·s^{-1}. Some examples of velocity distributions measured using different carriers are reported in Ref. 11: from the measured velocity distributions translational temperatures of O_2 in the beams are found to be in the 2–3 K range in all cases. Because of collisional relaxation during the expansion, O_2 molecules are expected to have very cold rotational and vibrational temperatures, and in particular the rotational temperature can not be much higher than the final translational temperature.[18] We estimate[11] that under present beam conditions over 95% of the molecules are slowly rotating in the ground state $K=1$, and the corresponding rotational angular momentum exhibits a strong spatial quantization. The large number of collisions between carrier gas atoms and seeded molecules, which occur during the beam formation, generate also an anisotropic distribution of the final rotational angular momentum along the beam velocity direction.[11,12] Therefore scattering data measured with such beams are more sensitive to features of the interactions—such as their anisotropy—than data taken in the configuration described in the previous section.

A key parameter in these experiments is the ratio $v/v_{\max}$ between the selected velocity v and the measured peak velocity $v_{\max}$ of the narrow velocity distribution of each seeded beam. Magnetic analysis of paramagnetic oxygen molecules

TABLE I. Weights W_M of the two helicity states $M=0$ and $M=1$.[a]

$v/v_{\max}$[b]	W_0	W_1
0.95	1/3	2/3
1.00	0.48	0.52
1.05	0.66	0.34
1.10	0.80	0.20

[a]These weights vary slightly for different mixtures of seeding gases (Ref. 11). More than 20 such mixtures were used in this work (Ref. 13); the entries in this table are those used in the analysis.
[b]See Sec. II C.

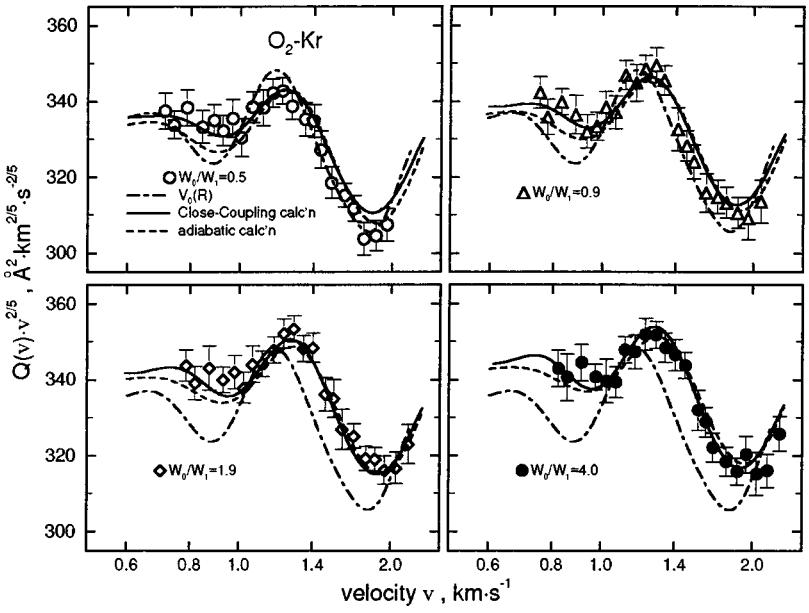

FIG. 4. Total integral cross sections, as in Fig. 2, for scattering of rotationally ''cold'' supersonic seeded beams of molecular oxygen by Kr atoms, at four different degrees of molecular alignment, given in terms of the indicated ratio W_0/W_1 (see Table I). Dotted-dashed lines are calculations for scattering by $V_0(R)$ as in previous Figs. 2 and 3, which have been reported for comparison; solid lines are CC calculations of total cross sections and dashed lines are the results of the adiabatic approach of Sec. III B.

in seeded supersonic beams has proved[11] a correspondence between the $v/v_{\max}$ ratio and the molecular alignment; in particular the polarization degree has been found to increase sensibly with increasing $v/v_{\max}$, favoring, at the higher $v/v_{\max}$ ratios, molecules flying with the plane of rotation parallel to the flux velocity direction. Since almost all the molecules are in the lowest $K=1$ rotational level, only the two *helicity* states $M=0$ or 1, where M is the absolute value of the projection of **K** along the velocity direction, are allowed.[19] After the supersonic expansion, the two helicity states are statistically populated in the tail of the velocity distribution, while the relative population of the $M=0$ state increases drastically with $v/v_{\max}$ and in a similar way for all carrier gases used.[11] In Table I are reported the weights W_M of the two helicity states $M=0$ and 1 for the $v/v_{\max}$ values relevant in present experiments.

The use of different gas carrier compositions allows us to vary v and to control the $v/v_{\max}$ ratio, and to measure cross sections as a function of v, at specified values of the alignment degree. Actually about 20 different gas mixtures have been used to adequately cover the whole velocity range.[13]

The relative ratios between cross sections, at $v/v_{\max}=0.95$, 1.00, 1.05 and 1.10, are measured with high accuracy in each run of data acquisition and as a function of collision velocity v.

Scattering cross sections on an absolute scale are obtained normalizing the average values for the $v/v_{\max}=0.95$ case (i.e., in the presence of a statistical mixture of the helicity states) to the average absolute value measured with the rotationally ''hot'' beam (see previous section). Results are reported in Figs. 4 and 5 for Kr and Xe targets, respectively.

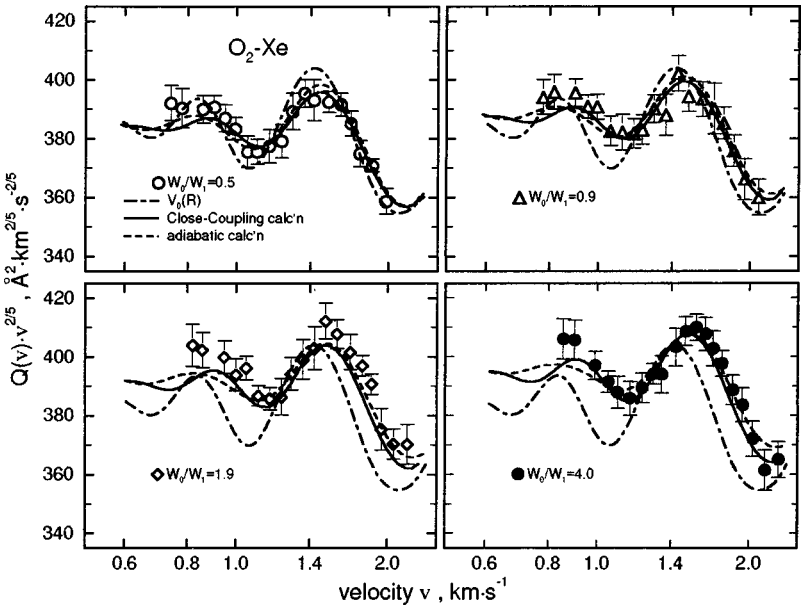

FIG. 5. Same as Fig. 4 for the Xe-O_2 system.

The observation is made that, with increasing $v/v_{\max}$, the scattering measurements—when compared with those obtained from the rotationally hot beam (see Figs. 2 and 3 and dotted-dashed lines in Figs. 4 and 5)—show both an increase in the average absolute value of the cross sections and a shift in the location of the glory extrema. These effects must be attributed to a manifestation of the anisotropy of the interaction potential, which operates between projectile molecule and target atom. Curves in the figures are calculations of the scattering cross sections according to procedures to be described further on in the following.

III. THEORY AND COMPUTATIONS

A. Cross section formulas

The interaction potential between Kr or Xe (considered as structureless atoms) and an oxygen molecule (modeled as a rigid rotor), depends on R, the distance between the atom and the center of mass of the diatom, and on the orientation angle θ which the molecular axis forms with respect to R $(0 \leqslant \theta \leqslant \pi)$. The neglect of vibrational and electronic degrees of freedom is justified by the low collision energies involved in these experiments.

The relevant quantum mechanical theory of atom-diatom collisions has been extensively studied.[20,21] In order to describe the collision process one has to solve, under scattering boundary conditions, a multichannel Schrödinger equation, at given total angular momentum J and energy E,

$$\left[\left(\frac{\hbar^2}{2\mu}\frac{d^2}{dR^2}+E\right)\mathbf{1}-\mathbf{V}^{J\,\epsilon}(R)\right]\mathbf{F}(R)=0, \tag{1}$$

where μ is the reduced mass of the collision complex and the potential energy matrix $\mathbf{V}^{J\,\epsilon}(R)$ is the representation of three operators,

$$\mathbf{V}^{J\,\epsilon}(R)=\mathbf{V}_{\rm rot}+\mathbf{V}_{\rm centr}+\mathbf{V}_{\rm int}, \tag{2}$$

in a suitable basis of eigenfunctions of J and parity ϵ. The three terms respectively represent the rotation of the diatomic molecule, with a moment of inertia I and rotational energy $\hbar^2K(K+1)/2I$ (only odd K values are allowed for O_2), the centrifugal operator, with eigenvalues $\hbar^2\ell(\ell+1)/2\mu R^2$—$\ell$ being the orbital angular momentum quantum number—and $\mathbf{V}_{\rm int}$ is the matrix element of a scalar function of R and θ, namely the interaction potential $V(R,\theta)$.

This quantum mechanical problem has been numerically investigated and the effectiveness of approximate solutions is now fully appreciated.[21] Cross sections can be obtained from solutions of Eq. (1), which provide the transition matrix $\mathbf{T}$ in the $|\ell K\rangle$ representation.

In general the integral cross section Q for a scattering process is obtained as a weighted sum of contributions of partial cross sections σ^J, each one corresponding to a particular value of the total angular momentum J. If the initial state of the diatom is $|KM\rangle$ (where M, as seen in Sec. II C, is the projection of $\mathbf{K}$ along the relative velocity direction) and the process concerns the formation of all $|K'\,M'\rangle$ substates of the same final level K', the partial cross section can be defined (see, for example, Ref. 22) as

$$\sigma^J_{KM,K'}=\left(\frac{\pi}{k_K^2}\right)\sum_{\ell,\ell'\bar{\ell}}(2J+1)i^{\bar{\ell}-\ell}[(2\ell+1)(2\bar{\ell}+1)]^{1/2}\times\begin{pmatrix}K & \ell & J\\ M & 0 & -M\end{pmatrix}\times\begin{pmatrix}K & \bar{\ell} & J\\ M & 0 & -M\end{pmatrix}T^J_{K\ell,K'\ell'}T^{J*}_{K\bar{\ell},K'\ell'}, \tag{3}$$

where k_K is the wave number of the system in the entrance rotational channel K, the terms in brackets are $3j$ symbols and ℓ, $\bar{\ell}$ and ℓ' take all the allowed values. The cross section $\sigma^J_{KM,K'}$ pertains to an elastic $(K=K')$ or rotationally inelastic $(K\neq K')$ processes. By summing over all J values the integral cross section is obtained,

$$Q_{KM,K'}=\sum_J \sigma^J_{KM,K'}. \tag{4}$$

If the molecular helicity state distribution W_M is controlled and several final states K' are accessible at the investigated collision energies, the total (elastic + inelastic) integral cross section Q_K is given by

$$Q_K=\sum_M W_M\sum_{K'} Q_{KM,K'}. \tag{5}$$

In the case of a statistical distribution of W_M values (no polarized molecules), the previous equation reduces to

$$Q_K=\frac{1}{2K+1}\sum_{K'} Q_{K,K'}, \tag{6}$$

where $Q_{K,K'}$ is given by

$$Q_{K,K'}=\left(\frac{\pi}{k_K^2}\right)\sum_{J,\ell,\ell'}(2J+1)|T^J_{K\ell,K'\ell'}|^2. \tag{7}$$

Present supersonic beam experiments involve O_2 molecules exclusively in the rotational ground state $K=1$, both projections $M=0$ and $M=1$ being possible, with weights W_M which change as a function of the molecular alignment degree. Therefore Eqs. (3), (4) and (5) will be used in the analysis of scattering results.

B. Adiabatic picture

To understand the origin of the observed anisotropic effects in the measured cross sections (see Sec. II C) and to clarify the collision dynamics of aligned molecules we have found it useful also to treat the collision process following an adiabatic representation in the coupled states framework.[7]

This representation considers the centrifugal energy in Eq. (2) as a diagonal term, so ℓ is a ''good'' quantum number and the collision is described as evolving along R-dependent effective adiabatic potential curves, obtained by properly taking into account the coupling of molecular rotations and the electrostatic interaction potential $V(R,\theta)$. These effective potentials adiabatically correlate to different states of the diatom in the triatomic complex, and correspond to free rotor states as $R\to\infty$, approaching libration modes at

short R values as the rotor becomes progressively hindered. They are defined in terms of K and its projection along R, which asymptotically correlates with the helicity M. The behavior of the adiabatic potential curves can be accurately predicted in the two limits by perturbation theory; for explicit formulas see Refs. 7 and 14.

The elastic component of the cross section is here defined as a weighted sum of the contributions relative to the scattering along each effective adiabatic potential. The weight factors depend on the rotational state of the molecule before the collision. Transitions between adiabatic states of different helicity, correlating with the same rotational level of the free rotor, can be induced by the Coriolis coupling at the crossings, i.e., where the anisotropy of the repulsion balances that of the attraction; such couplings depend on the impact parameter and on the collision velocity.

According to this description, nonadiabatic transitions, which represent passages between adiabatic curves of defined M character but belonging to different K, are responsible for inelastic events and are localized in restricted R ranges at intermediate intermolecular distances. They occur when the interaction anisotropy is of the same magnitude as the rotational energy, because then the hindered rotor states of the diatom transform into the libration states of the complex.[7] The probability of inelastic transitions depends on the features of the adiabatic potentials in the intermediate R range, on the asymptotic separation of the rotational levels and on the collision energy.

C. Semiclassical description

Experiments carried out with hot effusive beams (Sec. II B) exploit the collision dynamics of oxygen molecules fast rotating in high rotational levels and with their rotational planes randomly oriented. As suggested by the adiabatic representation (Sec. III B), the total cross sections so measured are mainly determined by elastic collisions since the energy splitting between two adjacent rotational levels increases with K, lowering the probability of inelastic events. Under such conditions the system can be viewed as a pseudoatom - atom case and the collision is mainly driven by the spherical component of the interaction $V_0(R)$. Thus, it is of interest to summarize the main formulas which describe elastic scattering by a central field potential, and to stress the connections between potential features and cross section properties. For collisions in systems with sufficiently high reduced mass, as the present ones, and in the thermal energy range, a semiclassical view of molecular scattering can be followed. The elastic cross section $Q(v)$, as a function of the relative collision velocity v, can be factored as[23]

$$Q(v)=\overline{Q}(v)+Q_{\mathrm{glory}}(v), \tag{8}$$

where $Q_{\mathrm{glory}}(v)$ is an oscillatory term, called the glory component, which depends on phase shifts associated with partial waves of intermediate orbital angular momentum ℓ values. From a semiclassical point of view they correspond to trajectories at intermediate impact parameters b and at nearly zero deflection angle, for which attraction and repulsion balance their opposite effects, interfering with trajectories at impact parameters so large that the effect of the potential is negligible. The high resolution measurements of the glory pattern represent a relevant experimental tool since it strictly depends on the features of the interaction in the potential well, in particular on the well depth ϵ and on its location R_m (Ref. 24).

The smooth (averaged) component of the cross section $\overline{Q}(v)$, which is mainly affected by collisions at small deflection angles, is determined by phase shifts associated with large ℓ (or large impact parameters). This component depends on the long range part of the interaction and in the case of a purely attractive potential, typically tending to $-C_6/R^6$, is given by[25]

$$\overline{Q}(v)=8.083\left(\frac{C_6}{\hbar v}\right)^{2/5}, \tag{9}$$

TABLE II. Interaction potential parameters for the Kr-O_2 and Xe-O_2 systems. The estimated uncertainties are ~5% for the well depth ϵ, ~2% for the well location R_m, ~10% for the long range constant C_0, ~5% and ~10% for the anisotropic A_2 and A_4 preexponential terms, respectively, and ~4% for the α coefficient.

	Kr-O_2	Xe-O_2
	$V_0(R)$	
ϵ (meV)	13.40	15.20
R_m (Å)	3.88	4.05
β	6.5	6.5
C_0 (meV Å^6)	$7.05\cdot10^4$	$1.02\cdot10^5$
x_1	1.12	1.12
x_2	1.55	1.55
	$V_2(R)$	
A_2 (meV)	$4.5\cdot10^6$	$8.4\cdot10^6$
α (Å^{-1})	3.37	3.37
a_2	0.26	0.26
	$V_4(R)$	
A_4 (meV)	$7.0\cdot10^5$	$1.0\cdot10^6$

TABLE III. Main features of the relevant cuts of the PES for the Kr-O_2 and Xe-O_2 systems. In the Table are also reported the characteristics of the isotropic V_0 terms. The well depth ϵ is in meV while the well location R_m and the zero σ of the potentials are given in Å.

		Kr-O_2	Xe-O_2
$V(\theta=0°)$	ϵ	10.80	12.94
	R_m	4.13	4.30
	σ	3.72	3.86
$V(\theta=45°)$	ϵ	13.05	14.81
	R_m	3.93	4.10
	σ	3.52	3.67
$V(\theta=90°)$	ϵ	15.84	17.87
	R_m	3.72	3.87
	σ	3.30	3.44
V_0	ϵ	13.40	15.20
	R_m	3.88	4.05
	σ	3.47	3.62

where $\hbar$ is the Planck constant $h/2\pi$ and the C_6 is the induced dipole-induced dipole long range constant. Accordingly, the measurement of the absolute value of the average cross section $\overline{Q}(v)$ provides information on the long range attraction.

To better identify the potential regions respectively probed by $\overline{Q}(v)$ and $Q_{\text{glory}}(v)$, it is necessary to note that the phase shift associated with each partial wave (or each trajectory) is mainly accumulated in the neighborhood of the classical distance of closest approach R_c. For a glory trajectory it lays between the location of the minimum of the well (R_m) and the distance (σ) where attraction and repulsion balance at short range.[26] The relevant R_m and σ values as obtained in the present analysis (see Sec. IV A and the Appendix) are reported in Tables II and III. Since semiclassically the relationship holds,

$$J+1/2=[2\mu(E-V(R_c))]^{1/2}R_c/\hbar, \tag{10}$$

a range of partial waves ℓ responsible for the glory effect can be identified. Similar considerations suggest that the $\overline{Q}(v)$ term mainly probes the attractive potential at an intermolecular distance of the order of $(\overline{Q}(v)/2\pi)^{1/2}$ (Ref. 27); again, the relevant partial waves can be easily identified. Although these ''rules of thumb'' strictly apply to central field scattering, they also will help to analyze the total cross sections due to anisotropic potential energy surfaces.

D. Exact and approximate calculations

A fast and accurate semiclassical method has been used to compute total cross sections from a central field potential, making use of a computer code based on the stationary phase approximation.[28] The calculation of scattering cross section including the full anisotropy required the use of extensive close coupling (CC) numerical techniques. We have used the MOLSCAT package[29] on an ALPHA AXP 2100 computer available at the Universidad Complutense de Madrid, with two modifications: (i) in order to obtain the cross sections for aligned molecules we have introduced a subroutine where Eq. (3) has been implemented; (ii) the present need of very high total angular momentum J values required implementation of a very stable subroutine for computing $3j$ coefficients.

The performances of the MOLSCAT code have been tested on a model for the Ar-N_2 system for which elastic and inelastic contributions are available from independent calculations.[30] A crucial point regarding the convergence of the calculations is the number of channels to be included in the CC expansion. The fully converged numerical solution of the Schrödinger equation for relatively heavy systems, such as the present ones, is prohibitively expensive; as a consequence, at the collision energies ($\approx 50-500$ meV) probed in these experiments a control of the optimal dimension of the calculations is necessary. The choice of the maximum J value which gives appreciable contribution to Q, and the number of coupled rotational channels at each J, proved to be essential. For the present systems we have found that the accurate calculation of the average component of the cross section $\overline{Q}$ requires summing over the contribution of $\sim 10^3$ partial waves, while it is sufficient to couple only the first five rotational channels ($K' \leqslant 9$) to correctly describe the glory effects measured with rotationally cooled ($K=1$) and aligned O_2 molecules. Numerical examples will illustrate these aspects in the next section.

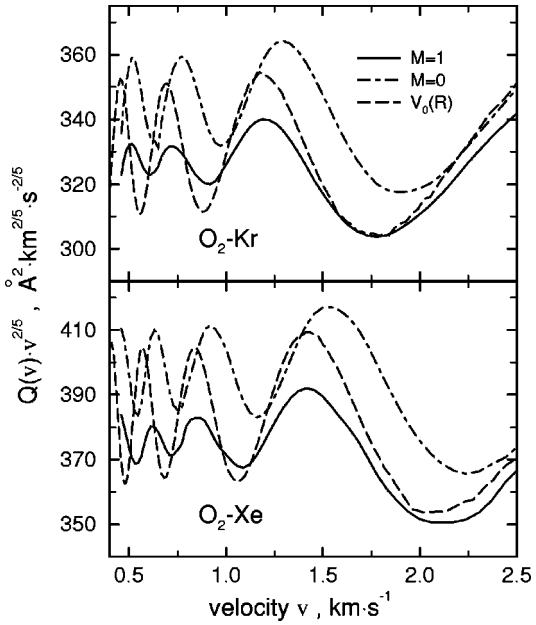

FIG. 6. CC total integral cross sections for both systems are reported as solid lines ($M=1$ helicity) and dotted-dashed lines ($M=0$ helicity). Results for elastic scattering by the spherical component $V_0(R)$ are also shown (dashed lines) for comparison. All calculations refer to the center-of-mass reference frame.

Total integral cross sections have been first calculated in the center-of-mass reference frame and then convoluted in the laboratory system, properly taking into account[31] the average on the experimental conditions used, to provide a direct comparison with the experimental results.

IV. DATA ANALYSIS AND DISCUSSION

A. The potential energy surfaces

For present atom-diatom systems the potential energy surface (PES) $V(R,\theta)$ is represented, as discussed in the Appendix, by a Legendre polynomial expansion including even terms, where the first radial coefficient $V_0(R)$ represents the spherical component of the interaction, while higher order terms define the anisotropic behavior of the PES. Functional forms parametrizing the $V_0(R)$, $V_2(R)$ and $V_4(R)$ terms used in this work are reported in the Appendix, together with a discussion of the criteria followed to obtain the best fit parameters. As already pointed out in Sec. II B, scattering cross sections, measured with a ''hot'' effusive beam, provide information on the spherical component $V_0(R)$, whose best fit parameters are reported in Table II. Cross sections, calculated using only this term, are compared with the experimental results in Figs. 2 and 3. The satisfactory reproduction of the measured glory pattern confirms the expectation that under such experimental conditions the scattering data are determined essentially by collisions from a central potential.

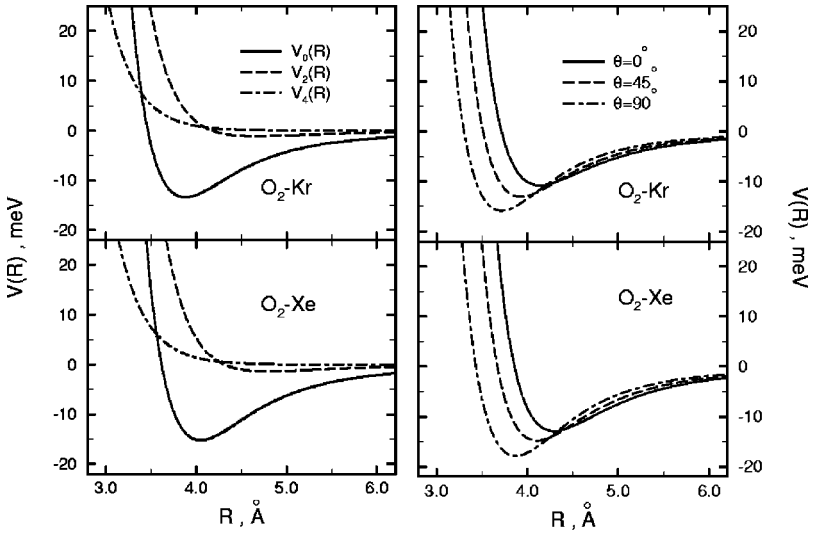

FIG. 7. The left panel shows potential energy terms V_0, V_2 and V_4 as a function of the intermolecular distance R for both studied systems, while the right panel reports cuts of the PES at three θ values. See also Appendix for parametrization and Table II for best fit potential parameters.

Figures 4 and 5 show the comparison between calculated cross sections from the V_0 potential and experimental data measured with molecular beams containing O_2 molecules rotationally cooled and at controlled alignment degrees. The evident disagreement suggests, as expected, that the latter experimental data are influenced by orientational and inelastic effects, as a manifestation of the anisotropy of the interaction.

Extensive CC scattering calculations, using PES parametrized as illustrated in the Appendix, have been performed for both systems, in order to account for the increase of the average cross section $\overline{Q}(v)$ and the shift of the glory extrema as the molecular alignment is increased. In this second step of the analysis only the parameters A_2, A_4, α and a_2—defining the features of anisotropic components V_2 and V_4 (see the Appendix)—have been varied. A_2, A_4 and α are obtained from the analysis of the glory shift, while a_2 from the increase of $\overline{Q}(v)$. The best fit potential parameters are reported in Table II, together with the estimated uncertainties, and the CC total integral cross sections for both helicities $M=0$ and $M=1$ are compared in Fig. 6 with those for scattering from the spherical component V_0 only. The weighted sum of contributions from different helicities (with weights as in Table I) provides the center-of-mass cross sections; calculated results in the laboratory frame are compared with the experimental data in Figs. 4 and 5. Potential terms V_0, V_2 and V_4 for both systems are plotted in the left panel in Fig. 7, while some cuts of the full PES are shown in the right panel, and relevant potential features are reported in Table III. In the following we report typical calculations of elastic and inelastic, partial and total scattering cross sections from the obtained PES, in order to get further insight on the dynamics for these systems. The main results, useful for present discussion, will be illustrated in the following.

B. Scattering from a central potential: The V_0 term

In the effusive beam, used in some of the present scattering experiments, rotationally excited O_2 molecules up to $K=41$ are present in an appreciable concentration (most populated levels correspond to $K=9-13$). However, in this collision energy range, the inelasticity of O_2 in $K=15$ is found to be four times smaller with respect to that for O_2 in $K=1$, confirming its decrease with the increase of the initial rotational level. For this reason all molecules in sufficiently high rotational states are expected to only undergo elastic collisions.

To control the validity of the procedure employed to characterize $V_0(R)$ (see above) we computed for Kr-O_2, using the complete PES, the CC cross sections $Q_{K,K'}$ [see Eq. (7)] with open channels K,K' corresponding to $K=9$ and $K'=9$ or $K=15$ and $K'=13,15,17$. The two calculations yield essentially similar results, undistinguishable in Fig. 2, where also are shown elastic cross sections (i.e., from the V_0 component only), and total (elastic + inelastic) cross sections from the anisotropic PES, considering the O_2 molecules randomly oriented in $K=1$. The comparison shows that scattering calculations from V_0 and from the anisotropic PES, taking O_2 in sufficiently high initial K levels, lead to identical positions for glory extrema, while the glory amplitude is slightly higher when anisotropy is neglected. However, the CC calculations which start from O_2 exclusively in $K=1$ are found to underestimate the glory amplitude and do not reproduce the glory extrema location. These observations confirm the reliability of the determination of the V_0 component from the analysis of the ''hot'' effusive beam scattering results.

C. The role of the interaction anisotropy

To get information on the collision dynamics of rotationally frozen ($K=1$) and aligned molecules and to determine which features of the PES are mainly responsible for the observed anisotropy effects in the measured cross section (see Sec. II C), it is useful to analyze, at a given collision velocity, the behavior of the CC partial cross sections $\sigma^J_{1\,M,K'}$, whose sum as in Eq. (4) yields the total integral cross section $Q_{1\,M,K'}$. We have chosen to examine, for both systems, two collision velocities, respectively corresponding to a glory maximum and a glory minimum: for Kr-O_2 these velocities are 707 and 1678 $m\cdot s^{-1}$, and for Xe-O_2 they are 707 and 1412 $m\cdot s^{-1}$. Collisions in the helicity state $M=1$ are considered here and the comparison with the $M=0$ case

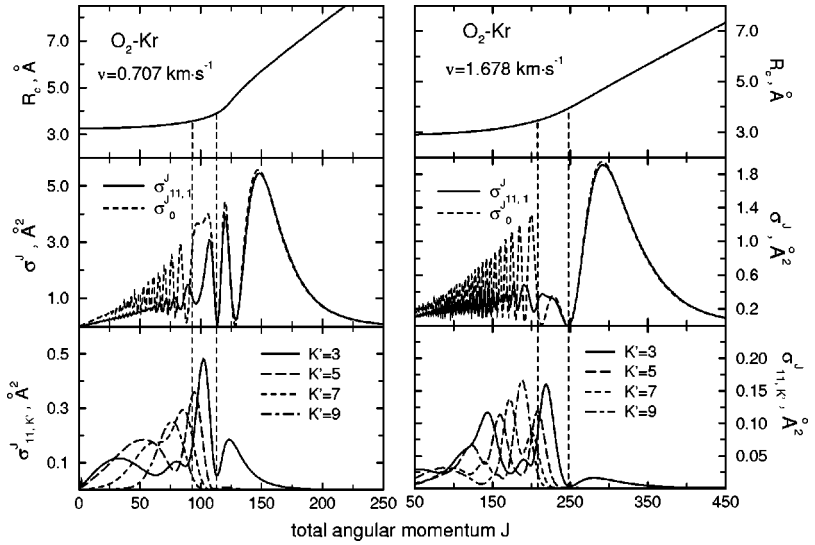

FIG. 8. Turning points R_c, elastic σ^J and inelastic components $\sigma^J_{1\,1,K'}$ (at the indicated K' values) of integral cross section as a function of angular momentum J, for the Kr-O_2 system, at collision velocities $v=707$ $m\cdot s^{-1}$ (corresponding to a maximum) and $v=1678$ $m\cdot s^{-1}$ corresponding to a minimum in the glory structure). Elastic and inelastic components refer to the $M=1$ helicity value and are obtained from CC calculations as explained in the text. Vertical lines define the J-range which mainly contributes to the glory undulations in the total cross section, see Sec. III C.

will be presented in Sec. IV E. Elastic $\sigma^J_{1\,1,1}$ and inelastic $\sigma^J_{1\,1,K'}$ components are reported in Fig. 8 for the Kr-O_2 case and in Fig. 9 for the Xe-O_2 case, together with results of exclusively elastic σ^J_0 cross sections, computed using only the spherical component $V_0(R)$. In the same figures the relationship between distance of closest approach R_c and angular momentum J is also reported.

Three J-ranges can be identified, on the basis of the different relative contribution to the observed effects in the measured cross sections when the molecular alignment degree is varied. In high J-range, inelastic processes are negligible and the scattering is governed by long range attraction, (large R_c). This J-range determines the average component of the total integral cross section $\overline{Q}(v)$. Variations in this component can then be ascribed to the long range splitting of the effective adiabatic potentials with respect to $V_0(R)$.

The glory interference effect arises from a narrow range of intermediate J values, whose boundaries can be calculated through the semiclassical formula of Eq. (10), taking into account that the corresponding R_c values must fall between the σ and R_m distance[26] (see Tables II and III). The boundaries of the intermediate range are indicated in Figs. 8 and 9 as vertical dashed lines: there inelastic transitions are due to the interaction anisotropy in the well region and rotational excitation to the lowest levels $K'=3,5,7,9$ are reported. In this J-range the elastic $\sigma^J_{1\,1,1}$ component provides values which are higher or lower than σ^J_0 in correspondence, respectively, of a minimum or a maximum in the glory interference pattern. (see Figs. 8 and 9). This illustrates that for $M=1$ collisions the main contribution to the observed quenching and shifting of the glory oscillations arises from inelastic events, operative in the same J-range, which remove flux from the elastic channel.

In the small J-range, inelastic transitions to higher K' levels become operative, although the elastic component $\sigma^J_{1\,1,1}$ still represents the largest contribution to the total cross section. Both the elastic $\sigma^J_{1\,1,1}$ and σ^J_0 components are fast oscillating as a function of J. They can be estimated using the venerable random phase approximation[32] and their contribution to Q is small. The difference between σ^J_0 and $\sigma^J_{1\,1,1}$ is due to inelastic effects, which affect large angle scattering

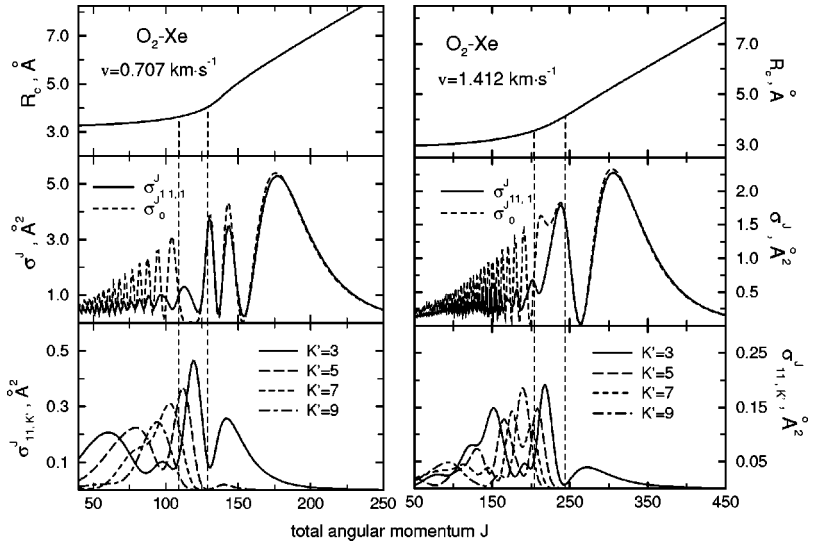

FIG. 9. Same as Fig. 9, for the Xe-O_2 system, at collision velocities $v=707$ (glory minimum) and 1412 $m\cdot s^{-1}$ (glory maximum).

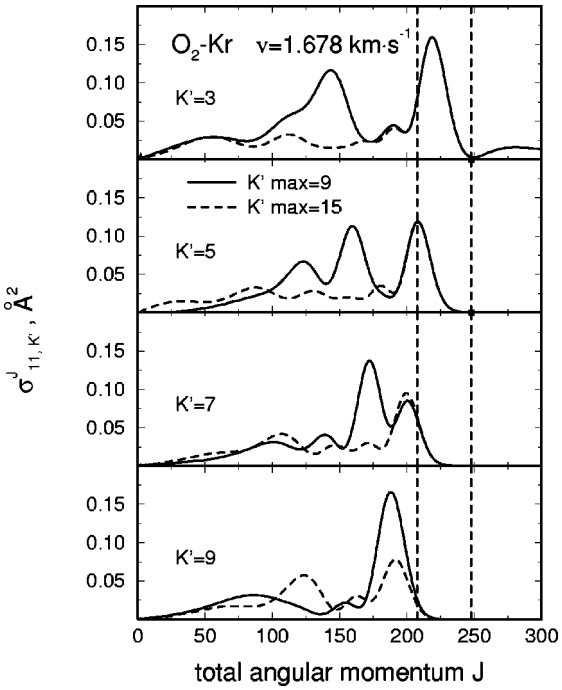

FIG. 10. Inelastic components $\sigma^J_{1\,1,K'}$ of integral cross section (at the indicated K' values) as a function of angular momentum J, for the Kr-O_2 system, at a collision velocity $v=1678\ \mathrm{m\cdot s^{-1}}$. They refer to $M=1$ helicity and are the results of CC calculations performed considering final levels opened up to $K'=9$ (solid lines) or 15 (dashed lines). Glory region boundaries are indicated by vertical lines.

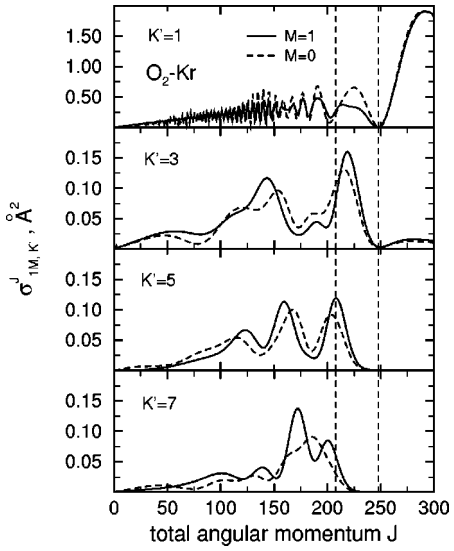

FIG. 11. Elastic and inelastic components $\sigma^J_{1\,M,K'}$ of integral cross section (at the indicated K' values) as a function of angular momentum J, for the Kr-O_2 system, at $v=1678\ \mathrm{m\cdot s^{-1}}$. They are the result of CC calculations performed considering final levels opened up to $K'=9$ and refer to $M=1$ (solid lines) and $M=0$ (dashed lines) helicity values. Glory region boundaries are indicated by vertical lines.

and probe short range interactions. They should be accessible to differential cross section measurements.

D. Coupled rotational channels

Figures 8 and 9 illustrate that in the intermediate J-range, as expected, the role of inelastic processes decreases as K' increases and only inelastic channels leading to $K'=3,5$ and 7 substantially contribute to alter glory pattern features. A similar conclusion was drawn from a previous analysis of Ar-O_2 scattering,[33] where O_2 was taken in $K=1$ and no helicity dependence considered. Therefore since in the present collision energy range many excited rotational levels (up to $K'\geqslant 40$) are accessible, the contribution of other inelastic channels must be confined within a lower J-range. Their influence is negligible on the glory pattern, but is crucial to define the behavior of differential cross sections at large scattering angles (see also above). To confirm this, we carried out further CC calculations of $\sigma^J_{1\,1,K'}$ for the Kr-O_2 system at a velocity of $1678\ \mathrm{m\cdot s^{-1}}$, considering opening of rotational levels up to $K'=15$. As is clearly shown in Fig. 10, the inelastic components $K=1,M=1\rightarrow K=3,5,7,9$ in the intemediate J-range (glory region) are not affected by the opening of further rotational channels. On the other hand, significant variations are observed in the small J-range, where partial inelastic cross sections are affected by opening further channels (up to $K'=15$), although the overall contribution to the total cross section is already convergent when only the first four excited channels (up to $K'=9$) are included. Actually the overall inelastic contribution to the total cross section $Q_{1\,1,K'}$ varies only from 35.97 $\mathrm{Å}^2$ (five rotational channels coupled, up to $K'=9$) to 36.08 $\mathrm{Å}^2$ (eight channels coupled up to $K'=15$).

E. Helicity dependence of the cross sections: The collision dynamics of aligned molecules

The present measurements have demonstrated the effect of the molecular alignment on the glory pattern. To provide a more quantitative analysis of this experimental evidence we have extensively carried out CC calculations for both the $M=0$ and 1 helicity states of $K=1$. Figure 11 shows results for $\sigma^J_{1\,1,K'}$ and $\sigma^J_{1\,0,K'}$ components of the Kr-O_2 system at $v=1678\ \mathrm{m\cdot s^{-1}}$. This comparison indicates that in the intermediate J region both elastic and inelastic components differ for the two helicities, in accord with the differences in the glory pattern between $M=0$ and $M=1$, which can be observed in Fig. 6. For the $M=1$ case, the higher probability for inelastic processes (see Fig. 11) results in a more pronounced glory quenching. The shift of the glory extrema position toward higher velocity and the lower inelastic probability found for the $M=0$ case indicate that the collision complex at intermediate J values and at distances close to R^J_c probes different portions of the PES as the molecular helicity is varied. The cut of the PES probed in the $M=0$ configuration is expected to exhibit a deeper well depth and to induce a smaller inelasticity.

To clarify this point and to fully understand the collision dynamics of the aligned molecules we have attempted a description of the shift and quenching of the glory pattern within the adiabatic approach of Ref. 7 (see Sec. III B). To reproduce the observed effects it is necessary to introduce, at crossings of the effective adiabatic potentials (i.e., when the interaction anisotropy changes sign: $\sim$ 4.2 and $\sim$4.4 Å for the Kr and Xe cases, respectively), a complete helicity mix-

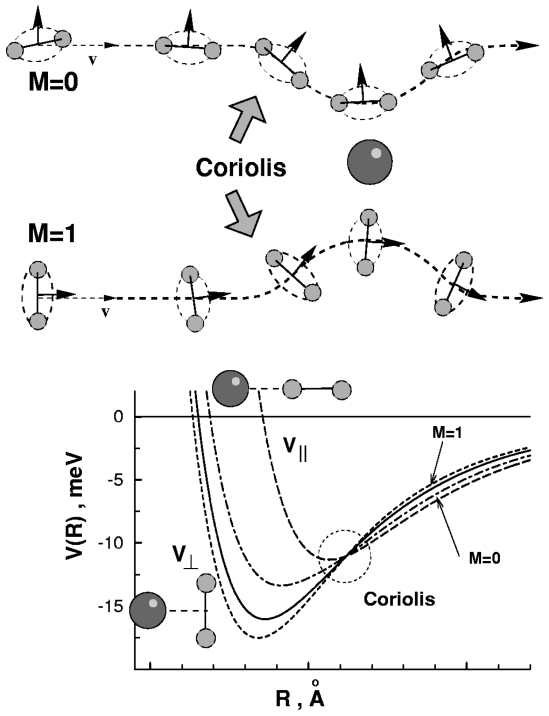

FIG. 12. A picture of ''glory'' trajectories for molecules with $M=0$ (edge-on) or $M=1$ (broadside) alignment. They evolve into perpendicular (''airplane'') or collinear (''pinwheel'') configurations, respectively, in the region of closest approach, where phase shifts attain their maximum, giving rise to the glory effect. The region where Coriolis coupling occurs (near the crossing between the two effective potential curves) is also shown. Solid and dotted-dashed lines represent effective adiabatic potentials for the interaction between Kr atoms and O_2 molecules (see Sec. III B), correlating at large R with helicity values $M=0$ and 1 of $K=1$ respectively; dashed and long dashed lines depict the interaction in the two limiting collinear and perpendicular configurations labeled as $V_{\|}$ and $V_{\perp}$, respectively.

ing (properly accounting for the parity states) induced by the Coriolis coupling, which originates a change in the collision complex configuration when the system follows the glory trajectory. Figure 12 shows that for $M=0$ the linear (''pinwheel'') configuration, dominant at long range, turns into a T-shape (''airplane'') configuration at shorter R. The ''airplane'' configuration is characterized by a higher bond energy and a lower rotational inelastic probability. An opposite behavior is effective for the $M=1$ case, for which an essentially linear (''pinwheel'') configuration, less stable and with a higher rotational inelasticity, describes the collision complex at distances close to the distance of closest approach.

Another important anisotropic effect measured in this work is the change of the average component of cross sections observed when the molecular alignment is increased. The adiabatic analysis suggests that the average component of cross sections for collisions with $M=0$ is higher than that for collisions with $M=1$ since the long range potential which drives the process depends, in the first case, more effectively on the collinear geometry. This geometry exhibits a long range attraction stronger with respect to the perpendicular one. Therefore the observed different behavior depends on the long range helicity splitting which, within the adiabatic representation,[7,14] is directly related to the anisotropic coefficient a_2 of the dispersion attractive potential (see Appendix).

V. FINAL REMARKS AND CONCLUSIONS

The main result of this work has been the accurate characterization of the full anisotropic potential energy surfaces for the Kr-O_2 and Xe-O_2 systems. This has been based on the analysis of effects such as the change of the relative value of the cross sections and the shifting and quenching of the glory extrema measured in scattering experiments carried out as a function of the degree of alignment of the projectile molecules.

Comparisons between experimental data and exact (CC) or approximate calculations have served to clarify the dynamics of the collisional process involving aligned molecules.

A final consideration concerns the validity range of the obtained PES. As discussed above, present experimental data are essentially determined by collisions at intermediate and large impact parameters which mainly depend on the attractive component of the interaction; therefore present PES are reliable essentially in the negative range, which includes the intermediate region where the well occurs: 3.5 Å$\leqslant R\leqslant$ 7.5 Å for Kr-O_2 and 3.6 Å$\leqslant R\leqslant$ 8 Å for Xe-O_2. The repulsive wall should be probed by different types of experiments such as elastic and inelastic differential cross sections at large scattering angles and at higher collision energies.

The ϵ and R_m values reported in Table II agree with and are thought to be more accurate than previous determinations from similar experiments available in the literature.[17] Values of the long range C_0 parameter (an effective induced multipole-induced multipole term) are, as expected, higher than *ab initio* results for the induced dipole-induced dipole C_6 constant recently proposed by Meath:[34] the latter are $\sim$30% smaller with respect to the C_0 values reported here. The long range anisotropy coefficient a_2 is also found to be 0.26, higher than 0.23, which corresponds to the case of a pure dipole-dipole attraction.[35] Both these increases are attributed to the appreciable role played by higher order multipole-multipole interactions in the R range probed by the average component of the cross sections.[36]

The same experimental technique has been recently applied to characterize the PES in the $O_2(^3\Sigma_g^-)-O_2(^3\Sigma_g^-)$ system where both van der Waals and spin-spin (chemical) interactions concur to define energy and structure of the tetratomic complex.[37]

While a main conclusion of this paper is to have established that scattering experiments with a controlled molecular alignment are an important tool for the characterization of anisotropic interaction potentials, a mirror perspective that emerges is to perform such experiments to probe the degree of alignment of the molecules in seeded beams for systems for which reliable intermolecular interactions are available. This aspect has been already illustrated in Ref. 14 and is currently being pursued for more complex systems, such as acetylene and benzene.

ACKNOWLEDGMENTS

This work is supported by the Italian National Research Council (CNR), by the Ministero dell'Università e della Ricerca Scientifica e Tecnologica (MURST), and by the European Union through the programs Training and Mobility of Researchers Network ''Potential Energy Surfaces for Molecular Spectroscopy and Dynamics'' (Contract No. ERB-FMRX-CT96-0088].

APPENDIX A: PARAMETRIZATION OF POTENTIAL ENERGY SURFACES

The PES $V(R,\theta)$ can be properly represented by a Legendre polynomial expansion,

$$V(R,\theta)=\sum_{n=0}^{\infty} V_n(R)\cdot P_n(\cos\ \theta), \tag{A1}$$

where only even terms need be considered when, as in the present case, the diatom is a homonuclear molecule. To analyze present scattering data, which depend on the intermediate and long range behavior of the PES, it has been sufficient to take only the first three terms of the expansion. Therefore $V(R,\theta)$ is here given as

$$V(R,\theta)\simeq V_0(R)+V_2(R)\cdot P_2(\cos\ \theta)+V_4(R)\cdot P_4(\cos\ \theta), \tag{A2}$$

where the isotropic $V_0(R)$ term represents the spherical component of the interaction, while the $V_2(R)$ and $V_4(R)$ coefficients define the interaction anisotropy. We used a MSV (Morse-spline-van der Waals) parameterization to represent the isotropic component $V_0(R)$. By scaling the distance and the energy, respectively, for the minimum location R_m and for the well depth ϵ,

$$x=\frac{R}{R_m},\quad f(x)=\frac{V_0(R)}{\epsilon}, \tag{A3}$$

we obtain, Morse

$$f(x)=\exp[-2\beta(x-1)]-2\exp[-\beta(x-1)]\quad \text{for } x\leqslant x_1, \tag{A4}$$

spline

$$f(x)=b_1+(x-x_1)b_2+(x-x_2)\times[b_3+(x-x_1)b_4]\quad \text{for } x_1<x<x_2, \tag{A5}$$

van der Waals

$$f(x)=-\left(\frac{C_0}{\epsilon R_m^6}\right)x^{-6}\quad \text{for } x\geqslant x_2. \tag{A6}$$

The β parameter, which defines the shape of the Morse function, is fixed to a value of 6.5 as characteristic of most van der Waals forces.[38] The x_1 and x_2 connecting points of the spline function are chosen, as for other previous cases,[14] in the neighborhood of 1.1 and 1.5, while b_1,b_2,b_3 and b_4—the spline parameters—are automatically fixed by imposing that the functions must have the same value and the same derivative at x_1 and x_2. Small variations of x_1 and x_2 introduce no significant change in the potential.

Total integral cross sections, measured in the thermal energy range as a function of the collision velocity, show a glory quantum interference structure, mainly sensitive to the features of the well depth located at intermediate R, overimposed to a smooth component whose value depends, as amply discussed in the text, on the strength of the long range attraction. Scattering data measured with ''hot'' effusive beams are mainly affected by the spherical component $V_0(R)$, therefore the MSV parametrization appears to be suitable for the present analysis since it allows to the independent varying of ϵ, R_m and C_0, which define, respectively, the main features of well depth and long range behavior of the involved interaction. Another important consideration concerns the long range attraction: the average cross section depends on the strength of the attractive potential in a defined range of R (see Secs. III and IV), where the R^{-6} induced dipole-induced dipole dispersion interaction gives the main contribution, even if higher order multipole interactions are not negligible. Therefore the C_0/R^6 term has the meaning of an effective dipole-dipole term since it describes the overall attraction in the distance range mainly probed by the experiment.

The anisotropic interaction $V_2(R)$ has been parametrized as

$$V_2(R)=A_2\cdot\exp(-\alpha R)-\frac{a_2\cdot C_0}{R^6}, \tag{A7}$$

where the exponential function describes the behavior of the short range repulsion and the second term represents the effect of the long range attraction. The last term is here defined as the product between the long range isotropic attraction $(-C_0/R^6)$ and the anisotropy coefficient a_2. Using Buckingham notation[39] we obtain the proper expression for a_2 in the case of pure dipole-dipole attraction,

$$a_2=\frac{\alpha_\parallel-\alpha_\perp}{\alpha_\parallel+2\alpha_\perp}, \tag{A8}$$

where $\alpha_\parallel$ and $\alpha_\perp$ are the collinear and perpendicular polarizabilities of the diatomic molecule; data in the literature lead to a value of $a_2\simeq 0.23$ (Ref. 35).

As discussed above, present scattering results depend on the attractive potential in a distance range where contributions from higher order terms (multipole-multipole interactions) are not negligible. Accordingly, the a_2 coefficients were chosen to vary, assuming $a_2=0.23$ as a lower limit. This is in view of the difficulty in disentangling the relative contribution of the dipole-dipole and multipole-multipole interactions to the overall anisotropic attraction in the probed intermolecular distance range. The final fits gave $a_2\simeq 0.26$.

The $V_4(R)$ term, parametrized as $A_4\exp(-\alpha R)$, has a smaller effect on the short range anisotropy and has been introduced to increase flexibility to the angular dependence of the PES.

[1] For a general review, see, for example, G. C. Maitland, M. Rugby, E. B. Smith, and W. A. Wakeham, *Intermediate Forces* (Clarendon, Oxford, 1981).

[2] For potential models see Ref. 1, and also, C. Doukatis, G. Scoles, S. Marchetti, M. Zen, and A. J. Thakkar, J. Chem. Phys. **76**, 3057 (1982); K. T. Tang and J. P. Toennies, *ibid.* **80**, 3726 (1984).

[3] V. Aquilanti, D. Cappelletti, V. Lorent, E. Luzzatti, and F. Pirani, J. Phys. Chem. **97**, 2063 (1993); V. Aquilanti, D. Cappelletti, and F. Pirani, J. Chem. Soc., Faraday Trans. **89**, 1467 (1993).
[4] R. Düren, in *Atomic and Molecular Beam Methods*, edited by G. Scoles (Oxford University Press, New York, 1988).
[5] U. Buck, Comments At. Mol. Phys. **17**, 143 (1986); J. M. Hutson, J. Chem. Phys. **89**, 4550 (1988); **91**, 4448 (1989); Annu. Rev. Phys. Chem. **41**, 123 (1990); F. A. Gianturco, J. P. Toennies, and M. Bernardi, J. Chem. Phys. **93**, 1641 (1990); L. Beneventi, P. Casavecchia, F. Pirani, F. Vecchiocattivi, G. G. Volpi, G. Brocks, A. van der Avoird, B. Heijmen, and J. Reuss, *ibid.* **95**, 195 (1991); L. Beneventi, P. Casavecchia, G. G. Volpi, C. C. K. Wong, and F. R. W. McCourt, *ibid.* **98**, 7926 (1993); F. A. Gianturco, F. Ragnetti, M. Faubel, B. Martinez-Haya, L. Y. Rusin, F. Sondermann, and U. Tappe, Chem. Phys. **200**, 405 (1995); A. Rohrbacker, K. C. Janda, L. Beneventi, P. Casavecchia, and G. G. Volpi, J. Phys. Chem. A **101**, 6528 (1997).
[6] V. Aquilanti, G. Liuti, F. Pirani, and F. Vecchiocattivi, J. Chem. Soc., Faraday Trans. 2 **85**, 955 (1989).
[7] V. Aquilanti, L. Beneventi, G. Grossi, and F. Vecchiocattivi, J. Chem. Phys. **89**, 751 (1988).
[8] K. H. Kramer, R. B. Bernstein, J. Chem. Phys. **40**, 200 (1964); S. Stolte, Ber. Bunsenges. Phys. Chem. **86**, 413 (1982); Z. Karny, R. C. Estler, and R. N. Zare, J. Chem. Phys. **69**, 5199 (1978); A. Mattheus, A. Fischer, G. Ziegler, F. Gottwald, and K. Bergmann, Phys. Rev. Lett. **56**, 712 (1986); H. J. Loesch and A. Remscheid, J. Chem. Phys. **93**, 4779 (1990); B. Friedrich and D. R. Herschbach, Nature (London) **353**, 412 (1991).
[9] R. B. Bernstein, D. R. Herschbach, and R. D. Levine, J. Phys. Chem. **91**, 5365 (1987).
[10] L. Zandee and J. Reuss, Chem. Phys. **26**, 327 (1977); H. Thuis, S. Stolte, and J. Reuss, *ibid.* **43**, 351 (1979); S. Stolte, in *Atomic and Molecular Beam Methods*, edited by G. Scoles (Oxford University Press, New York, 1988); H.-G. Rubahn and J. P. Toennies, J. Chem. Phys. **89**, 287 (1988).
[11] V. Aquilanti, D. Ascenzi, D. Cappelletti, and F. Pirani, Nature (London) **371**, 399 (1994); J. Phys. Chem. **99**, 13 620 (1995). The convention adopted in the present paper, more appropriate for the analysis of scattering experiments, implies that the weight of the state of helicity $M=1$, W_1, is *twice* the corresponding quantity in these references, while W_0 is the same.
[12] For relevant work on collisional alignment, see, M. P. Sinha, C. D. Caldwell, and R. N. Zare, J. Chem. Phys. **61**, 491 (1975); D. P. Pullman and D. R. Herschbach, *ibid.* **90**, 3881 (1989); D. P. Pullman, B. Friedrich, and D. R. Herschbach, *ibid.* **93**, 3224 (1990); J. Phys. Chem. **95**, 8118 (1991); H. J. Saleh and A. J. McCaffery, J. Chem. Soc., Faraday Trans. **89**, 3217 (1993); M. J. Weida and D. J. Nesbitt, J. Chem. Phys. **100**, 6372 (1994); E. B. Anthony, W. Schade, M. J. Bastian, V. M. Bierbaum, and S. R. Leone, *ibid.* **106**, 5413 (1997); S. Harich and A. Wodtke, *ibid.* **107**, 5983 (1997).
[13] V. Aquilanti, D. Ascenzi, D. Cappelletti, S. Franceschini, and F. Pirani, Phys. Rev. Lett. **74**, 2929 (1995).
[14] V. Aquilanti, D. Ascenzi, D. Cappelletti, R. Fedeli, and F. Pirani, J. Phys. Chem. **101**, 7648 (1997).
[15] T. Nenner, H. Tien, and J. B. Fenn, J. Chem. Phys. **63**, 5439 (1975); **64**, 3902 (1976); F. Pirani and F. Vecchiocattivi, *ibid.* **66**, 372 (1977).
[16] P. Kusch, J. Chem. Phys. **40**, 1 (1964); F. von Busch, Z. Phys. **193**, 412 (1966); H. Pauly and J. P. Toennies in *Methods Experimental Phys. A* **7**, 227 (Academic, London, 1968); P. Dehmer and L. Wharton, J. Chem. Phys. **57**, 4821 (1972); J. J. H. van Biessen, in *Atomic and Molecular Beam Methods*, edited by G. Scoles (Oxford University Press, New York, 1988).
[17] E. Luzzatti, F. Pirani, and F. Vecchiocattivi, Mol. Phys. **34**, 1279 (1977).
[18] A. Amirav, U. Even, J. Jortner, and L. Kleinman, Chem. Phys. **73**, 4217 (1980); J. Mettes, B. Heijmen, J. Reuss, and D. C. Lainè, *ibid.* **87**, 1 (1984); T. Matsumoto and K. Kuwata, Chem. Phys. Lett. **171**, 314 (1990).
[19] Note that the ground state of the O_2 molecule is actually split into three spin-rotational levels by the coupling between the electronic spin and the rotational angular momenta. Magnetic analysis yields the distribution of the magnetic sublevels of the spin-rotational states and angular momentum algebra (see Ref. 11) gives the actual populations of the helicity states in the beam. The latter are the quantities relevant for the analysis of present scattering data, since during the collision the electrostatic intermolecular interaction is large enough to decouple rotational and spin angular momenta even at large intermolecular distances.
[20] A. M. Arthur and A. Dalgarno, Proc. R. Soc. London, Ser. A **256**, 540 (1960); see *Atom-Molecule Collision Theory: A Guide for the Experimentalist*, edited by R. B. Bernstein (Plenum, New York, 1979), especially chapters by S. Stolte and J. Reuss, J. C. Light, D. J. Kouri, and D. Secrest.
[21] P. McGuire and D. J. Kouri, J. Chem. Phys. **60**, 2488 (1974); R. T Pack, *ibid.* **60**, 633 (1974); R. B. Walker and J. C. Light, Chem. Phys. **7**, 84 (1975); D. Secrest, J. Chem. Phys. **62**, 710 (1975); J. M. Launay, J. Phys. B **9**, 1823 (1976).
[22] M. H. Alexander, P. Dagdigian, and A. E. DePristo, J. Chem. Phys. **66**, 59 (1977).
[23] See, for example, M. S. Child, *Molecular Collision Theory* (Academic, London, 1974).
[24] R. B. Bernstein and T. J. P. O'Brien, Discuss. Faraday Soc. **40**, 35 (1965); R. B. Bernstein and T. J. P. O'Brien, J. Chem. Phys. **46**, 1208 (1967).
[25] R. B. Bernstein and K. H. Kramer, J. Chem. Phys. **38**, 2507 (1963).
[26] E. F. Greene and E. A. Mason, J. Chem. Phys. **57**, 2065 (1972); *ibid.* **59**, 2651 (1973).
[27] G. B. Ury and L. J. Wharton, J. Chem. Phys. **56**, 5832 (1972).
[28] F. Pirani and F. Vecchiocattivi, Mol. Phys. **45**, 1003 (1982).
[29] J. M. Hutson, S. Green, MOLSCAT computer code, distributed by Collaborative Computational Project No. 6 of the Engineering and Physical Sciences Research Council (UK), available on the worldwide web at http://www.giss.nasa.gov/molscat/.
[30] D. C. Clary, J. N. L. Connor, and H. Sun, Mol. Phys. **49**, 1139 (1983).
[31] G. Liuti, E. Luzzatti, F. Pirani, and G. G. Volpi, Chem. Phys. Lett. **135**, 387 (1987).
[32] H. S. W. Massey and C. B. O. Mohr, Proc. R. Soc. London, Ser. A **141**, 434 (1933); *ibid.* **144**, 188 (1934).
[33] M. S. Bowers, M. Faubel, and K. T. Tang, J. Chem. Phys. **87**, 5687 (1987).
[34] A. Kumar, W. J. Meath, P. Bündgen, and A. J. Thakkar, J. Chem. Phys. **105**, 4927 (1996).
[35] P. W. Langhoff, R. G. Gordon, and M. Karplus, J. Chem. Phys. **55**, 2126 (1971).
[36] This aspect has been also pointed out in the analysis of total integral cross section experiments performed with polarized NO beams in H. Thuis, S. Stolte, and J. Reuss, Chem. Phys. **43**, 351 (1979); and H. H. W. Thuis, S. Stolte, J. Reuss, J. J. H. van Biesen, and C. J. N. van den Meijdenberg, *ibid.* **52**, 211 (1980).
[37] V. Aquilanti, D. Ascenzi, M. Bartolomei, D. Cappelletti, S. Cavalli, M. de Castro, and F. Pirani (in preparation).
[38] V. Aquilanti, D. Cappelletti, and F. Pirani, Chem. Phys. **209**, 299 (1996).
[39] A. D. Buckingman, Adv. Chem. Phys. **12**, 107 (1967).